Experimental Study and Simulation of Concentration of Hydrogen Peroxide by Pervaporation Using Nafion®-Silica Nanocomposite Membranes

Nguyen Huu Hieu[1, 2*]

[1] Faculty of Chemical Engineering, School of Semiconductor and Chemical Engineering, Chonbuk National University, Jeonju, Jeonbuk 561-756, Republic of Korea.
[2] Key Laboratory of Chemical Engineering and Petroleum Processing, , Ho Chi Minh City University of Technology, VNU-HCMC, 268 Ly Thuong Kiet Street, District 10, Ho Chi Minh City.

* Corresponding author. Tel.: 0918498177; email: nhhieubk@hcmut.edu.vn
Manuscript submitted December 29, 2016; accepted March 24, 2017.
doi: 10.17706/ijmse.2017.5.1.1-15

Abstract: Nafion®-silica nanocomposite membranes were used to concentrate hydrogen peroxide by pervaporation to aid the development of improved membranes. Membranes were fabricated by casting Nafion® solution in dimethylformamide with colloidal silica. Their morphologies and thermomechanical properties were characterized with respect to silica content (5–20 wt%) by transmission electron microscopy, scanning electron microscopy, and dynamic mechanical analysis. Pervaporation was carried out using a feed solution of 70 wt% hydrogen peroxide at 30 °C and a permeate pressure of 0.5 Torr; the membranes were assessed with respect to permeate flux and selectivity. Permeate flux decreased slightly from 6.189 to 5.750 mol/(h·m^2) with increasing silica content; selectivity was increased by 60% compared with recast Nafion® without silica. Parameters for batch-type pervaporation process design, such as the retentate hydrogen peroxide concentration and the yield, were calculated using a mathematical model developed based on a solution-diffusion mechanism. The simulation results demonstrated that the modified Nafion® membranes should require smaller areas and improve pervaporation.

Keywords: Hydrogen peroxide, modeling, nafion®, pervaporation, silica, simulation.

1. Introduction

Hydrogen peroxide (H_2O_2) is an effective and non-polluting oxidant that is widely used in industry [1]. Most H_2O_2 is currently produced by anthraquinone oxidation (AO) to yield crude H_2O_2 (25 – 45 wt%), which is then concentrated to commercial grades[2]. Further concentration of aqueous H_2O_2 gives high test peroxide (HTP) at 85 to 98 wt%. Upon contact with a catalyst, HTP rapidly decomposes into hot steam and oxygen, a property that has been used to propel rockets [1]-[3]. H_2O_2 is most widely concentrated by vacuum distillation, which is inherently dangerous, though less dangerous than regular distillation, because it should deal with a high-concentration H_2O_2 vapor. A safer, pervaporation (PV)-based, membrane separation process, patented by NASA, that employs Nafion® and polysulfone membranes [4] uses high concentration H_2O_2 in only the liquid phase.

PV employs permselective membranes for the separation of liquid mixtures by partial vaporization (Fig. 1). A feed mixture contacts one side of the membrane at atmospheric pressure, and vapor permeate is collected on the other side by a vacuum pump or sweep gas [5]-[6]. Transport across the membrane is

driven by chemical activity differences that are established by the partial pressure differences of a species between each side of the membrane [5]-[6].

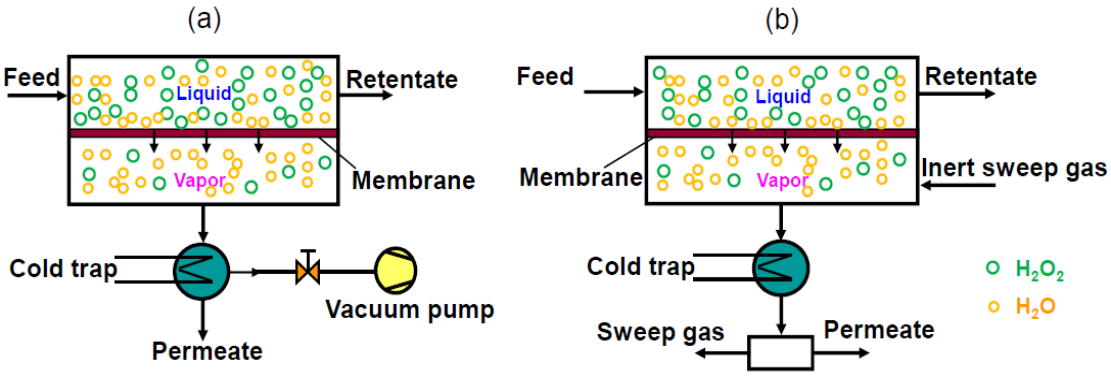

Fig. 1. PV employing: (a) vacuum pump and (b) sweep gas.

Nafion® membranes (Fig. 2) have been used in polymer electrolyte membrane fuel cells and in PV separations (Table 1). Its polytetrafluoroethylene backbone gives Nafion® thermal and chemical stability and hydrophobicity. Its sulfonic acid groups aggregate to form hydrophilic clusters [7]-[8] that can allow small molecules such as water or H_2O_2 to cross the membrane, giving Nafion® membranes applicability for concentrating H_2O_2. However, they show low selectivity (2.4) [4], indicating that Nafion® allows the transportation of H_2O_2 and water, which reduces the efficiency of PV separation. To reduce H_2O_2 permeability, membranes with high selectivity and improved separation performance are desired.

Modification of Nafion® by incorporating hydrophilic nanofillers, such as SiO_2, TiO_2, ZrO_2, zeolites, has been made for improving the performance of fuel cells [20]. For concentrating H_2O_2, the incorporation of these nanofillers into the Nafion® matrices can also be expected to improve the performance of pervaporation process. Since the presence of nanofillers which can reduce the diffusion of molecules in the filled membrane, leading to a reduction of the total permeation flux [21]. If the water permeation flux can be maintained and, thus enhancing the membrane selectivity.

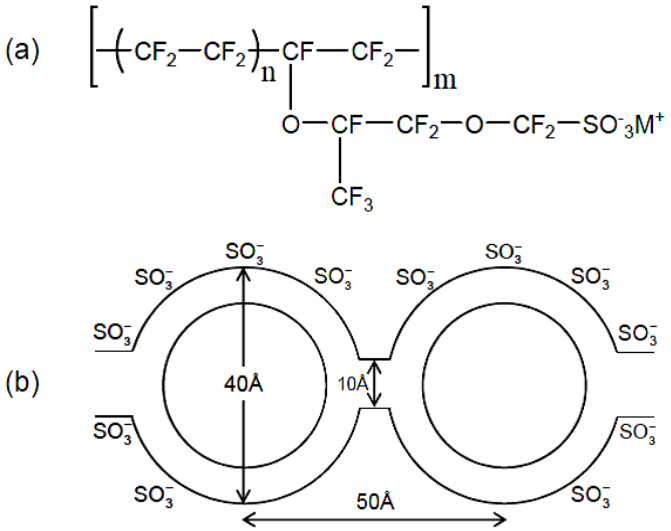

Fig. 2. Nafion®: (a) structure and (b) cluster network model. M^+ represents either a metal cation in the neutralized form or H^+ in the acid form.

Table 1. Applications of Nafion® membranes in PV

PV Processes	Mixtures	References
Concentration of aqueous solutions	hydrogen peroxide	[4]
	sulfuric acid	[9]
	iodic acid	[10]-[11]
	nitric acid	[12]-[13]
	acetic acid	[14]
	glycerine	[15]
	Isopropanol	[15]-[17]
	Methanol	[17]
	iodic acid/iodine	[18]
Organic/organic separation	methanol/triglyme	[19]

This work reports the use of a hygroscopic inorganic oxide filler, silica, added to the polymer matrices to give modified Nafion® membranes. Nanocomposite membranes were prepared by casting Nafion® solution in dimethylformamide (DMF) with colloidal silica. The membranes were characterized by transmission electron microscopy (Bio-TEM), scanning electron microscopy (SEM), and dynamic mechanical analysis (DMA). The effects of silica content on the membranes' PV performances were assessed.

To calculate the design parameters for batch-type PV systems, a mathematical model was developed based on a solution-diffusion mechanism for permeate flux that allowed optimum silica content to be calculated so as to facilitate the fabrication the nanocomposite membranes for improved H_2O_2 purification.

2. Experimental

2.1. Materials

A 5 wt% Nafion® solution in mixture of lower aliphatic alcohols and water (Dupont, equivalent weight 1100 g/mol SO_3H) was from Aldrich. Colloidal silica (30 wt% SiO_2, 10 – 20 nm particle size, SS-SOL 30) was from S-Chemtech. N,N-Dimethylformamide was from Samchun Pure Chemical Co., Ltd., Korea. H_2O_2 solution (70 wt%) was from OCI Co., Ltd., Korea. Deionized water was used in all experiments.

2.2. Membrane Preparation

Nafion®-silica nanocomposite membranes (Fig. 3) were produced by evaporating stirred Nafion® solution in a hood at 100 °C for 1 h until the Nafion® solution became a solid resin. The resin was dried in a vacuum oven at 100 °C for 3 h to complete solvent removal (i.e. lower aliphatic alcohols and water). The solid Nafion® was redissolved in DMF in the hood at 120 °C under vigorous stirring for 1 h to form about 7 wt% Nafion® in DMF solution. Various amounts of colloidal silica were homogeneously mixed with the Nafion®-DMF solutions by ultrasonication for 3 h. The nanocomposite membranes were prepared by casting the mixed solutions using a glass mold. The solutions were dried in a convection oven at 100 °C for 6 h until most of the solvent had evaporated and then for another 3 h at 130 °C. Finally, samples were annealed at 150 °C for 3 h. The resulting membranes were removed from the mold by adding deionized water and drying in a vacuum oven (750 mmHg) at 100 °C for 3 h.

Nanocomposite membranes with 0, 5, 10, 15, 20, and 25 wt% silica compared with the dry nanocomposite membrane were denoted as NS0, NS5, NS10, NS15, NS20, and NS25, respectively. NS25 was very brittle and could not be used for PV. All the cast membranes were ca. 120 μm thick. The membranes with silica loadings above 5 wt% were not transparent and were slightly more rigid than the neat Nafion® membrane.

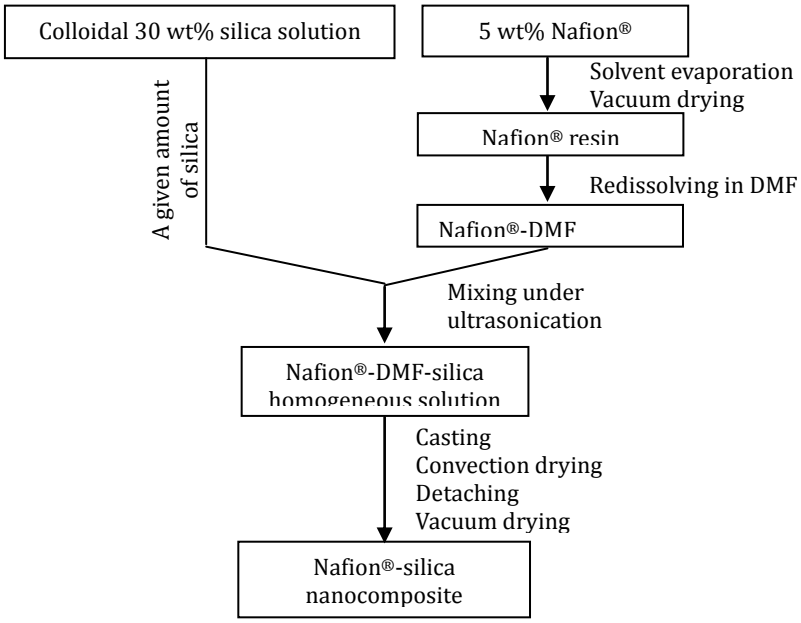

Fig. 3. Preparation of Nafion®-silica nanocomposite membranes.

2.3. PV Apparatus and Measurements

In the batch-type PV system (Fig. 4), membranes were placed on porous metal plate supports inside the membrane module. The feed solution was maintained at constant temperature in the module using an electric heating jacket equipped with a temperature controller. During testing, the permeate pressure was maintained by a vacuum pump, and monitored by a pressure gauge. PV conditions were controlled and monitored by computer (Table 2). The permeate vapor was condensed using pure ethanol at -40 °C; it was collected and weighed at intervals. Retentate and permeate H_2O_2 concentrations were measured using a refractometer. Each experiment was repeated three times under similar conditions.

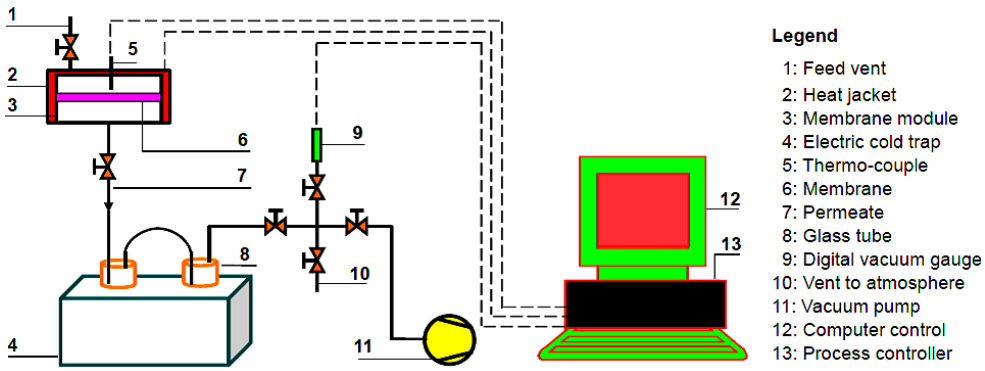

Fig. 4. The Batch-type PV apparatus.

Table 2. Experimental Conditions for Batch-Type PV

Parameters	Values
Membrane area (m^2)	6.486×10-3
Feed volume (mL)	200
Feed H_2O_2 concentration (wt%)	70
Feed temperature (^oC)	30
Permeate pressure (Torr)	0.5
Time period (h)	3

2.4. PV Performance Parameters

PV performance was evaluated from the total permeate flux (J_T) (mol/(h·m^2)) and the membrane selectivity (α) as follows:

$$J_T = \sum J_i = \frac{\dot{n}_P}{A} \quad (1)$$

$$\alpha = \frac{J_W}{J_H} = \frac{y_W}{y_H} \quad (2)$$

where J_i is the partial permeate flux for species i (mol/(h·m^2)), $\dot{n}_P$ is the total molar flow rate of permeation (mol/h), A is the membrane area (m^2), and y is the mole fraction on the permeate side. H and W denote H_2O_2 and water, respectively.

2.5. Characterization

Membranes' surfaces and cross-sections were observed by SEM (JEOL JSM-6400, Japan). Tapping-mode atomic force microscopy was used to examine their surface morphologies. Specimens were prepared for cross-sectional analysis by cryogenic fracturing in liquid nitrogen (77 K) and coating with gold by sputtering in a vacuum for 100 s. SEM images were then obtained at 0.2–40 kV.

Samples' morphologies were also studied by Bio-TEM (Hitachi H-7650, Japan) after they had been cut to 70 nm-thick slices using an ultramicrotome (Leica Ultracut UCT, Germany) at -80 °C with a diamond knife. The slices were collected on TEM grids (400 mesh Ni grids) and observed at 40–120 kV.

Membranes' thermomechanical properties were investigated with a dynamic mechanical analyzer (TA Instruments DMA Q800, USA) using a tension film clamp at 40 – 200 °C with 5 °C/min heating. Rectangular samples were cut with widths of 5.3 mm. Samples were measured under 30 μm tensile deformation oscillating sinusoidally at 1 Hz with a preload force of 0.01 N. Mechanical responses were analyzed through storage and loss moduli. Membranes' glass transition temperatures (T_g) were assessed from either the discontinuity of the storage modulus vs. temperature curve or the peak of the loss modulus vs. temperature curve.

3. Modeling

3.1. Permeation Equation

There are many models that predict molecular mass transfer through membranes. Of which, the solution-diffusion mechanism has been widely used in describing PV transport, including its preferential sorption, diffusion, and evaporation steps (Fig. 5) [22].

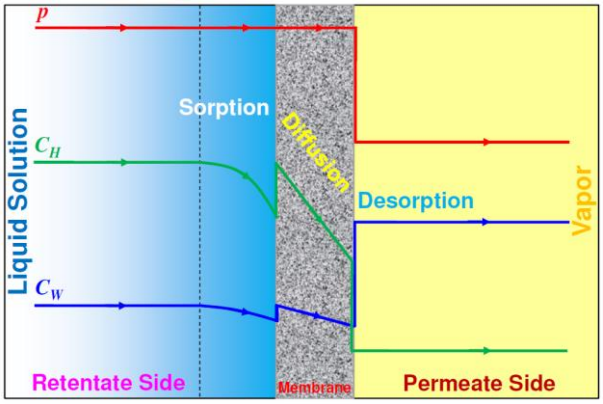

Fig. 5. Concentration and pressure profiles through a membrane.

It uses the following equation to describe the permeate flux of species i (Ji):

$$J_i = k_i \Delta p_i = k_i \left(\gamma_i x_{R,i} p_i^o - y_i p_P \right) \tag{3}$$

where k_i is the permeation coefficient for species i (mol/(h·m²Torr)), which is experimentally estimated; Δp_i is the difference in partial pressure of species i between the feed (or retentate) and the permeate sides of the membrane, the driving force for PV; γ_i is the activity coefficient; $x_{R,i}$ is the mole fraction on the retentate side; p_i^o is the saturated vapor pressure (Torr); and p_P is the permeate pressure (Torr).

The activity coefficients of H_2O_2 (γ_H) and water (γ_W) can be calculated by the following equations [23].

$$\gamma_H = exp\left\{ \frac{x_{R,W}^2}{RT} \left[B_0 + B_1 \left(3 - 4x_{R,W} \right) + B_2 \left(1 - 2x_{R,W} \right) \left(5 - 6x_{R,W} \right) \right] \right\} \tag{4}$$

$$\gamma_W = exp\left\{ \frac{x_{R,H}^2}{RT} \left[B_0 + B_1 \left(1 - 4x_{R,W} \right) + B_2 \left(1 - 2x_{R,W} \right) \left(1 - 6x_{R,W} \right) \right] \right\} \tag{5}$$

where B_0 = -1017 + 0.97T, B_1 = 85, and B_2 = 13, R = 1.987 (cal/(K·mol)) is the universal gas constant, and T is the absolute temperature (K).

The saturated vapor pressures of pure H_2O_2 and water can be calculated by the following equations [24].

$$logp_H^o = A_H + \frac{B_H}{T} + C_H logT + D_H T \tag{6}$$

$$logp_W^o = A_W + \frac{B_W}{T} + C_W logT + D_W T + ET^2 + FT^3 + GT^4 \tag{7}$$

where AH = 44.576, BH = -4025.3, CH = -12.996, DH = 4.6055×10-3, AW = 19.301, BW = -2892.3, CW = -2.8927, DW = -4.9369×10-3, E = 5.6069×10-6, F = -4.6458×10-9, G = 3.7874×10-12, p_H^o and p_W^o in mmHg.

Substituting into (3) and establishing a ratio of the permeate fluxes of H_2O_2 and water can give the mole fraction of H_2O_2 on the permeate side, y_H, by solving the following quadratic equation.

$$ay_H^2 + by_H + c = 0 \tag{8}$$

where $a = (k_W - k_H)p_P$, $b = \gamma_W x_{R,W} k_W p_W^o + \gamma_H x_{R,H} k_H p_H^o + (k_H - k_W)p_P$, and $c = -\gamma_H x_{R,H} k_H p_H^o$.

3.2. Material Balances

The flat sheet membrane module for batch-type PV (Fig. 6) with H_2O_2 solution feeds to the atmospheric-pressure upstream (retentate) side of the membrane. The downstream (permeate) side is under vacuum. Water molecules are removed preferentially over H_2O_2 from the solution by permeation through the membrane. They are then desorbed into the vapor phase on the permeate side.

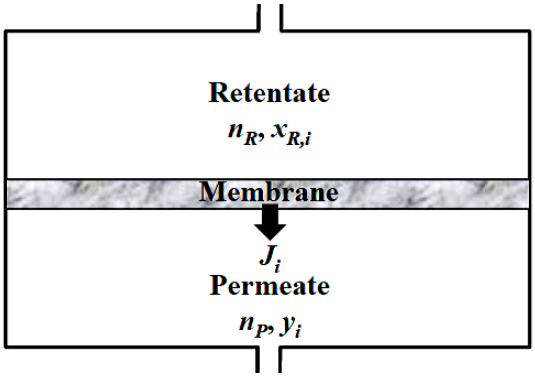

Fig. 6. Flat sheet membrane module for batch-type PV.

The molar balance for batch-type PV can be described by the following partial differential equation:

$$\frac{dn_R}{d\mathrm{t}} = -J_T A \tag{9}$$

where n_R is the number of moles of H_2O_2 solution on the retentate side (mol), and t is the operating time (s).

Assuming constant permeate flux during the short time interval Δt = 1 s, and for a given membrane area, A, integrating (9) can give the change of the number of moles of H_2O_2 solution on the retentate side.

$$\Delta n_{R,\mathrm{t}} = -J_{T,\mathrm{t}} A \Delta \mathrm{t} \tag{10}$$

After any time interval from the start, Δt, the number of moles of H_2O_2 solution on the retentate side,n_R, can be determined from the overall molar balance of the membrane module as follows:

$$n_{R,\mathrm{t}+\Delta \mathrm{t}} = n_{R,\mathrm{t}} + \Delta n_{R,\mathrm{t}} = n_{R,\mathrm{t}} - J_{T,\mathrm{t}} A \Delta \mathrm{t} \tag{11}$$

At t = 0, $n_{R,0} = n_F$ is the number of moles of feed solution.

The mole fraction of H_2O_2 on the retentate side can be calculated as follows:

$$x_{R,H,\mathrm{t}+\Delta \mathrm{t}} = \frac{x_{R,H,\mathrm{t}} n_{R,\mathrm{t}} - y_{H,\mathrm{t}} J_{T,\mathrm{t}} A \Delta \mathrm{t}}{n_{R,\mathrm{t}} - J_{T,\mathrm{t}} A \Delta \mathrm{t}} \tag{12}$$

At t = 0, $x_{R,H,0} = x_{F,H}$ is the mole fraction of H_2O_2 in feed solution.

PV's yield is given by:

$$Y = \frac{n_{R,H,\mathrm{final}}}{n_{R,H,\mathrm{initial}}} \times 100\% \tag{13}$$

where $n_{R,H,\mathrm{final}} = x_{R,H,\mathrm{final}}\, n_{R,\mathrm{final}}$ is the final number of moles of H_2O_2 on the retentate side and $n_{R,H,\mathrm{initial}} = n_{F,H} = x_{F,H} n_F$ is initial number of moles of H_2O_2 on the retentate side or the number of moles of H_2O_2 in the feed solution.

4. Simulation

Simulations for predicting the required membrane area, the PV's yield, and the concentration of H_2O_2 on the retentate side to produce 1 kg HTP (95 wt%) solution (Fig. 7) were carried out for each nanocomposite membrane. Based on the experimental data, the permeation coefficients of H_2O_2 and water, k_H and k_W, were calculated by (3). The input parameters for simulation, x_F,H, T, and p_P, were chosen to be the same experimental conditions (Table 2). For the calculation time interval Δt = 1 s, the procedure was started with using the input parameters to calculate the activity coefficients of H_2O_2 and water, γ_H and γ_W, by (4) and (5). Their saturated vapor pressures, p_H^0 and p_W^0, were calculated by (6) and (7). These parameters were used to obtained the mole fractions of H_2O_2, y_H, and water, y_W, on the permeate side from (8) and 1-y_H, respectively. The differences of partial pressure, Δp_i, and partial permeate fluxes, J_i, were obtained from (3). The total permeate flux, JT, was determined from (1). The estimated membrane areas and numbers of moles of feed H_2O_2 solution were used to calculate the change of the number of moles of H_2O_2 solution on the retentate side, Δn_R, and the number of moles of H_2O_2 solution on the retentate side, n_R, and the mole fraction of H_2O_2 on the retentate side, $x_{R,H}$, by (10), (11), and (12), respectively. n_R and $x_{R,H}$ were then

returned as the input parameters to repeat the calculation with increasing time periods up to 10 h. Finally, PV's yield was determined from (13). Output parameters of the model, including membrane area, yield, and retentate concentration of H_2O_2 were obtained.

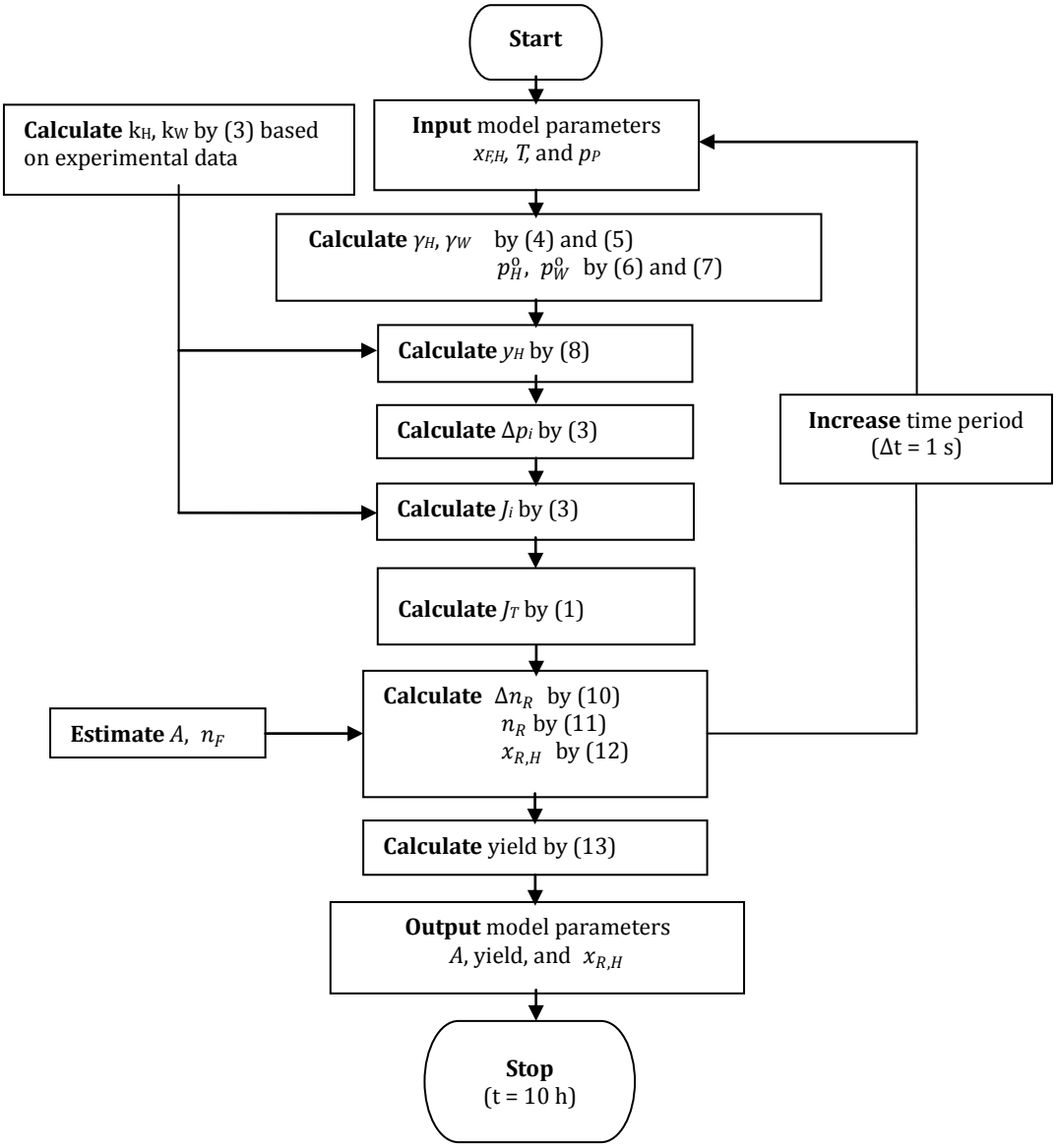

Fig. 7. Flowchart of simulation procedure.

5. Results and Discussion

5.1. SEM, TEM, and Thermomechanical Characterizations

SEM images (Fig. 8) show that all the nanocomposite membranes contained silica nanoparticles on their surfaces, though with the surfaces of NS5 and NS10 being smooth and similar to that of NS0, indicating homogenous dispersions of silica nanoparticles within Nafion® polymeric matrices. The membranes with high silica contents (NS15 and NS20) were rough, despite having relatively uniform distributions of silica nanoparticles. Agglomeration and segregation of the silica in the membranes' cross-sections increased with increasing silica content. Fine dispersions of the colloidal nanosilica particles could not be achieved at above 10 wt% loading.

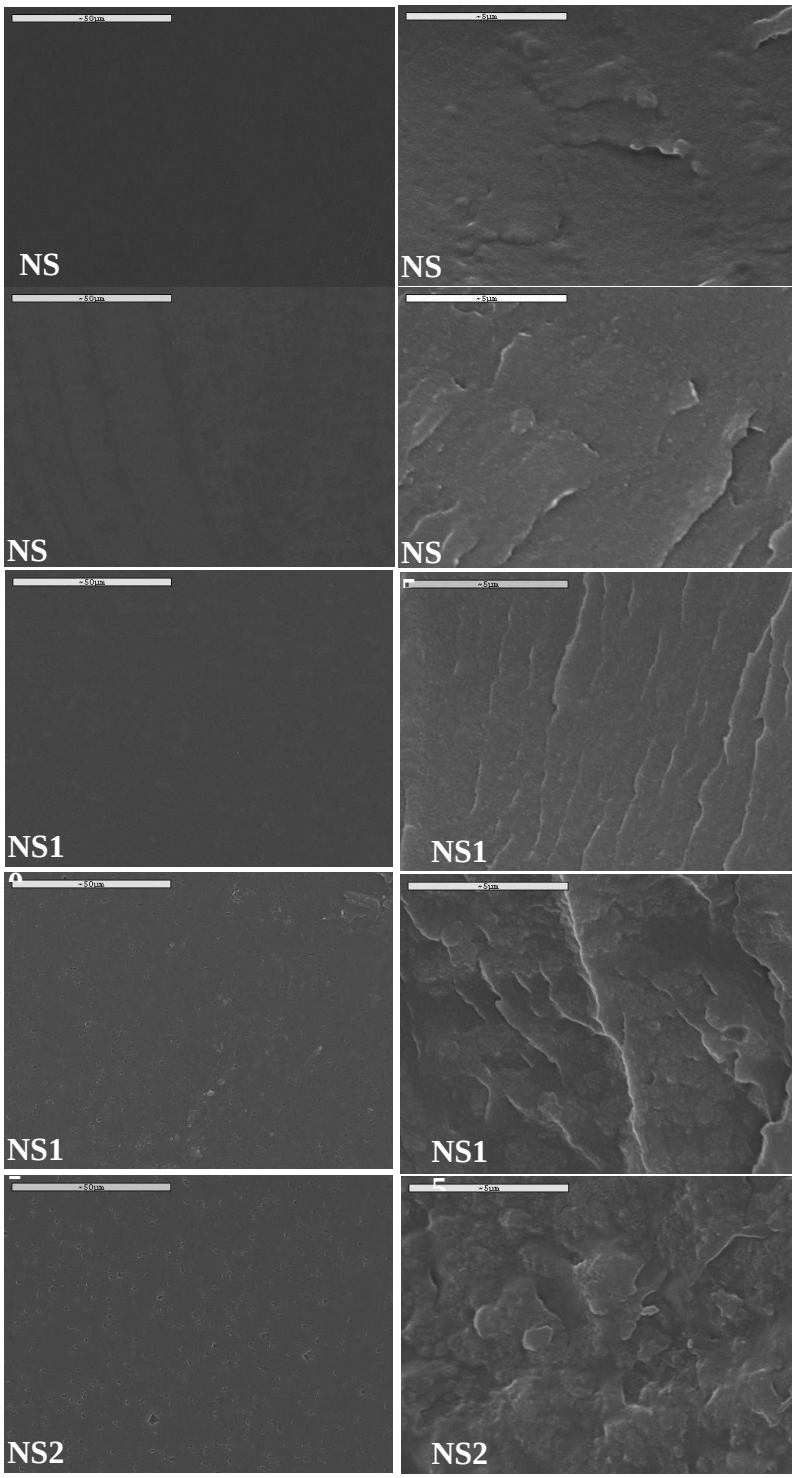

Fig. 8. Surface (left, scale bar: 50 μm) and cross-section (right, bar: 5 μm) SEM images of Nafion®-silica nanocomposite membranes.

The membranes' detailed structures are observable in the TEM images (Fig. 9). NS0 showed a homogeneous structure; the nanocomposite membranes showed relatively fine dispersions of SiO_2 nanoparticles within their polymer matrices. The silica nanoparticles were relatively similar between samples, being consistently ca. 20 nm in size. Agglomerations of silica nannoparticles became more common at higher concentrations of colloidal nanosilica. The images show that the distribution of the colloidal silica particles was not random; they tended to be dispersed in certain areas. Ionic moieties have

been reported to form clusters in ionomers such as Nafion® (Fig. 2) and it is likely that the hygroscopic colloidal nanosilica interacted with ionizable moieties and located in the ionic clusters rather than in hydrophobic regions.

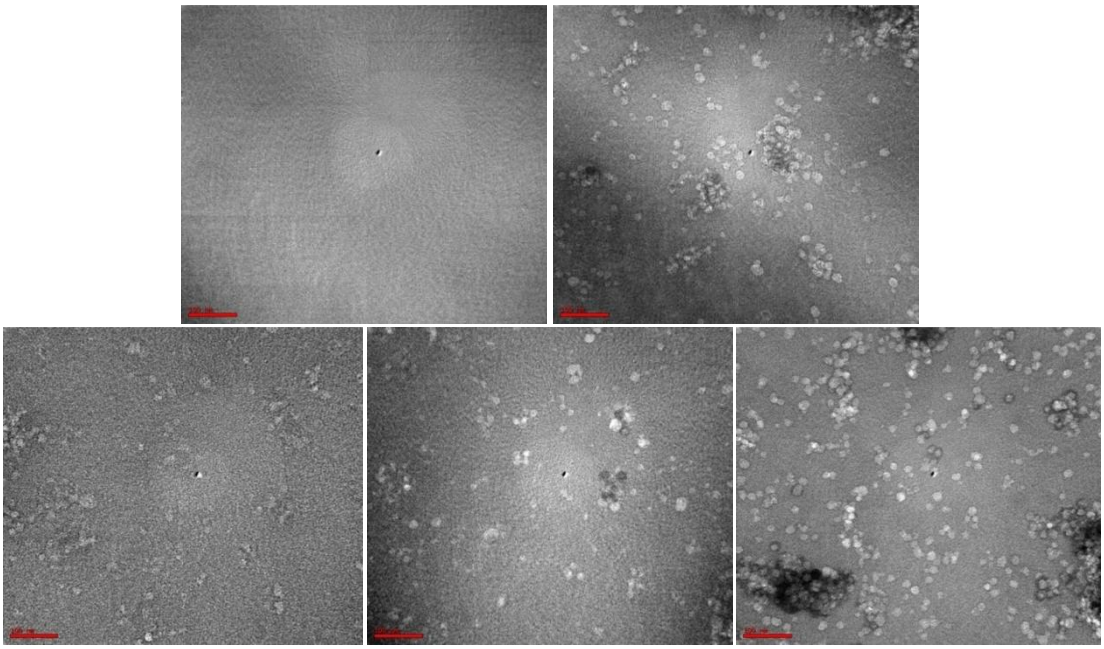

Fig. 9. TEM images (scale bar: 100 nm) of Nafion®-silica nanocomposite membranes.

DMA was carried out to investigate the membranes' thermomechanical properties with respect to temperature (Fig. 10). Storage modulus increased proportionally with silica loading, i.e. the membranes were stiffened by the silica. The glass transition of ionic clusters occurred at 90 – 120 °C and T_g increased with increasing silica content (Table 3). Both of these effects were directly related to molecular confinement of ionizable moieties in the Nafion® through interactions with the silica nanoparticles, which reduced the mobility of the polymer chains. This is consistent with previous reports of silica filler increasing the T_g of nanocomposite membranes [25].

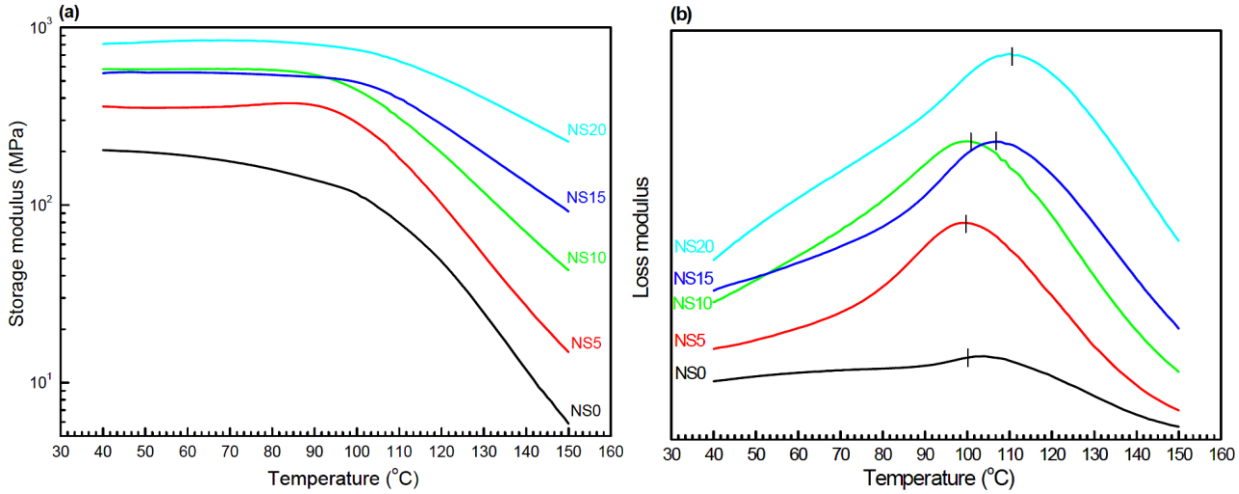

Fig. 10. (a) Storage (a) and (b) loss moduli of Nafion®-silica nanocomposite membranes with respect to temperature.

Table 3. Glass Transition Temperatures of Nafion®-Silica Nanocomposite Membranes Determined by Dynamic Mechanical Analysis

Membranes	Glass transition temperatures, T_g (°C)
NS0	100
NS5	102
NS10	104
NS15	106
NS20	110

5.2. Effect of Silica Content on PV Performance

Mean permeate fluxes (J_i) were calculated using (1) (Fig. 11); they initially increased and then decreased with membranes' increasing of silica content. The initial increase was due to membranes' increasing hydrophilicity with increasing hygroscopic silica content. The subsequent decrease with increasing silica content was likely due to the colloidal silica preferentially locating in the ionic clusters, reducing the transfer of water and H_2O_2 molecules through the membrane (Scheme 1). Simultaneously, resisting the swelling of nanocomposite membranes can also contribute to reduce the partial permeate fluxes. The maximum permeate flux observed in Fig. 11 may be explained in terms of sorption and diffusion parameters of the dual mode model for permeation of filled membrane proposed by Barrer (1984) [21]. However, the permeate flux of water remained higher than that of H_2O_2 because the saturated vapor pressure of water molecules is higher and their molecular size is smaller than those of H_2O_2. Therefore, water could more easily pass through the membranes, enhancing their selectivity (Fig. 12).

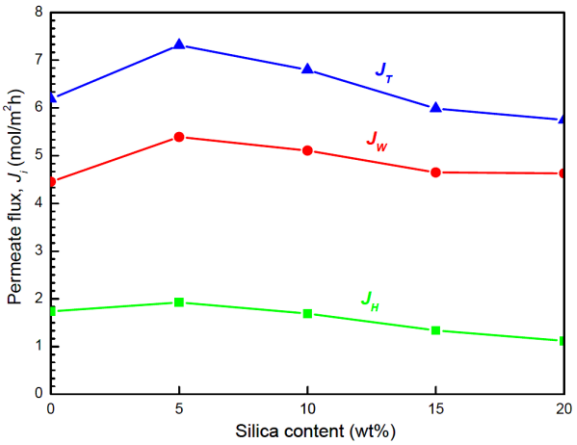

Fig. 11. Effect of silica contention permeate flux for the concentration of 70 wt% H_2O_2 at 30 oC and 0.5 Torr permeate pressure.

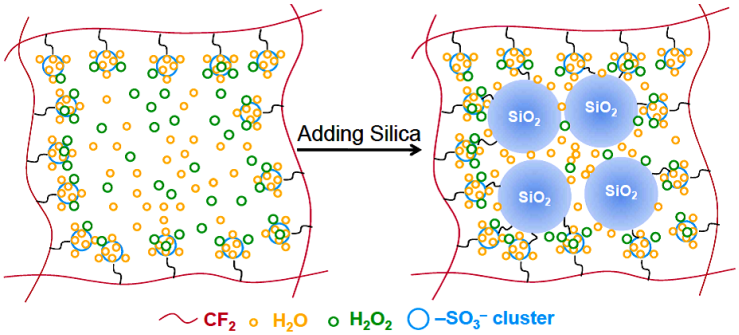

Scheme 1. The transport mechanism and the structure of Nafion®-silica nanocomposite membranes.

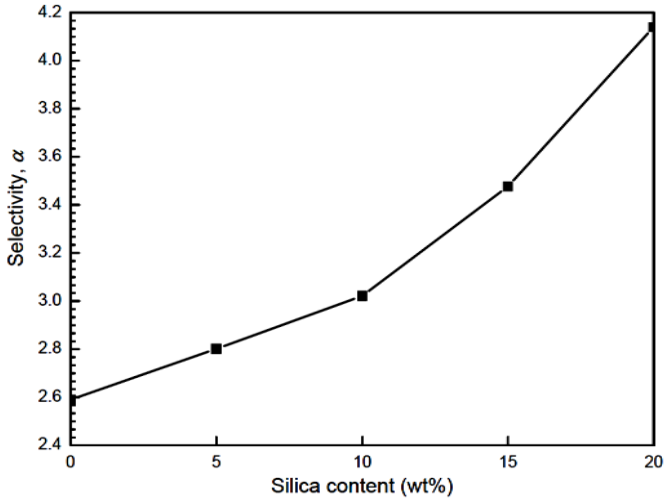

Fig. 12. Effect of silica content on membrane selectivity for the concentration of 70 wt% H_2O_2 at 30 °C and 0.5 Torr permeate pressure.

Selectivity was significantly increased from the 2.590 shown by NS0 to 4.139 shown by NS20. The observed selectivity of NS0 was consistent with that of the Nafion® membrane (2.4) reported in NASA's patent [4]. Nafion® membranes' PV performances were improved by the introduction of silica (Fig. 11 and Fig. 12).

5.3. Prediction Parameters

The membranes showed higher permeation coefficients, ki, for H_2O_2 than water (Table 4), indicating their stronger affinity towards H_2O_2 than water. This was likely due to hydrogen peroxide's greater dipole moment that allowed greater H-bonding with the membranes [1]. However, water molecules adsorbed and diffused easily across the membranes because of their physical properties, as described above. Therefore, water preferentially permeated through the membranes. The permeation coefficients also increased and then decreased with increasing silica content for similar reasons as permeate flux.

Table 4. Permeation Coefficients of Nafion®-Silica Nanocomposite Membranes for the Concentration of 70 wt% H_2O_2 at 30 °C and 0.5 Torr Permeate Pressure

Membranes	Permeation coefficients (mol/(h·m²Torr))	
	k_H	k_W
NS0	1.4740	0.5344
NS5	1.8588	0.5413
NS10	1.5184	0.5599
NS15	1.2133	0.4974
NS20	1.0229	0.4896

Silica content affected the membrane area required and the process yield (Fig. 13), with NS5 showing the largest required membrane area and the lowest yield and NS20 showing the highest yield and lowest required membrane area. H_2O_2 concentration on the retentate was predicted with respect to operating time (Fig. 14); NS20 showed the best performance and NS5, the worst. The same results were also obtained when carrying out the simulation with the calculation time interval Δt = 1 min. These simulation results provide an estimation of the effects of silica content on the design parameters and the membranes' performances during the PV concentration of H_2O_2 at specific operating conditions.

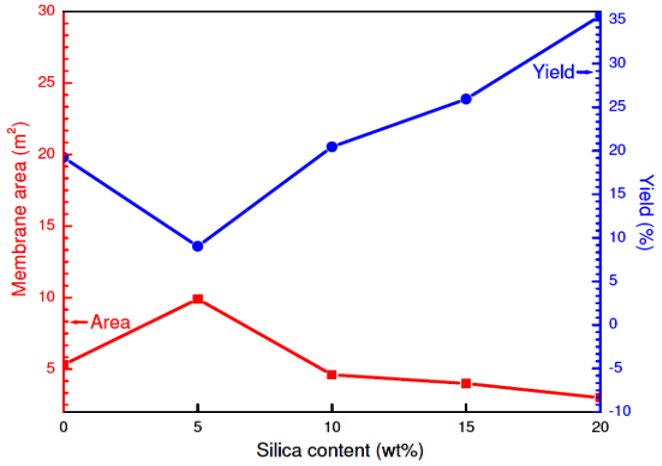

Fig. 13. Predicted membrane area and yield with respect to silica content.

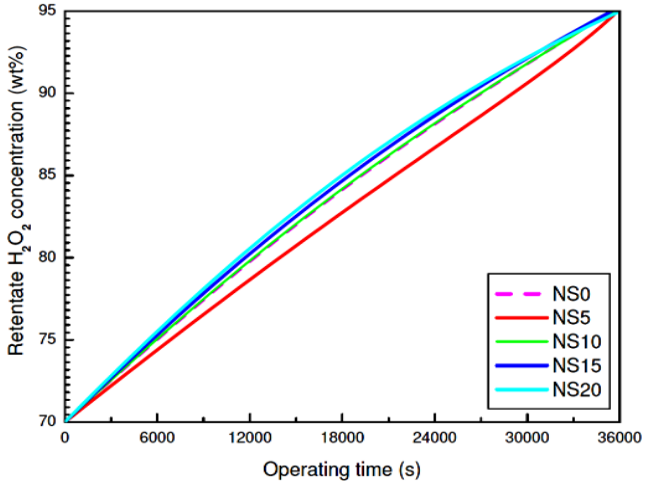

Fig. 14. Predicted retentate H_2O_2 concentration vs. operating time.

6. Conclusions

Nafion®-silica nanocomposite membranes for the concentration of H_2O_2 were prepared by casting. SEM and TEM images showed the fine distributions of silica nannoparticles in the Nafion® polymer matrices. DMA demonstrated that the colloidal silica nanoparticles increased the membranes' T_g.

The effects of silica contents on PV were investigated. Nanocomposite membrane with 20 wt% silica loading showed 7% lower total permeate flux and 60% increased selectivity compared with unfilled Nafion®. The addition of silica nanoparticles was shown to improve the PV performance of Nafion® membranes.

The production of 1 kg HTP (95 wt%) from a feed solution of 70 wt% H_2O_2 was calculated to assess the required membrane area, process yield, and retentate H_2O_2 concentration of each membrane. 20 wt% silica loading reduced the required membrane area to 3.0 m^2 and gave 35.51% yield, compared with the unfilled membrane's 5.3 m^2 area and 19.23% yield. Therefore, the cost of concentrating hydrogen peroxide can be reduced through improvements in membrane performance effected by adding silica to the Nafion®.

Assessing the effects of operating conditions on PV performance of the optimized membrane, including feed temperature and permeate pressure, will constitute subsequent investigation so as to optimize the operating conditions for the concentration of H_2O_2.

Appendix

Nomenclature	
Notations	
A, B, C, D, E, F, G	coefficients or constants
A	membrane area, m^2
a, b, c	coefficients
d	differential representation
J	permeate flux, mol/(h·m^2)
N	number of moles, mol
$\dot{n}$	molar flow rate, mol/h
k	permeation coefficient, mol/(h·m^2Torr)
p	pressure, Torr or mmHg
R	universal gas constant, cal/(K·mol)
T	temperature, K
t	temperature, ^oC
T	operating time, h or s
x	mole fraction in feed solution or on retentate side
Y	Yield
y	mole fraction on permeate side
Greek letters	
α	selectivity
γ	activity coefficient
Superscripts	
O	saturated vapor
Subscripts	
F, P, R	feed, permeate, and retentate
G	Glass
H	hydrogen peroxide
I	species
T	Total
W	Water

References

[1] Giorgio, D. F., Gennadiy, I., & Michael, W. (2011). Recent advances in catalytic asymmetric epoxidation using the environmentally benign oxidant hydrogen peroxide and its derivatives. *Chem. Soc. Rev., 40(3)*, 1722-1760.

[2] Dittmeyer, R, Grunwaldt, D. J., Pashkova, A. (2015). A review of catalyst performance and novel reaction engineering concepts in direct synthesis of hydrogen peroxide. *Catalysis Today, 248,* 149–159.

[3] Ventura, M., Wernimont, E., Heister, S., & Yuan, S. (2007). Rocket Grade Hydrogen Peroxide (RGHP) for use in Propulsion and Power Devices-Historical Discussion of Hazards. In *Proceedings of the 43rd AIAA/ASME/SAE/ASEE Joint Propulsion Conference & Exhibit*. Cincinnati: American Institute of Aeronautics and Astronautics.

[4] Parrish, C. F. (2006). *Concentration of Hydrogen Peroxide*. U.S. Patent 7,122,166 B2.

[5] Baker, R. W. (2012). Overview of membrane science and technology. In R. W. Baker (Ed.), *Membrane Technology and Applications* (pp. 1-14). New York: John Wiley & Sons, Ltd.

[6] Basile, A., Figoli, A., & Khayet, M. (2015). *Pervaporation, Vapour Permeation and Membrane Distillation: Principles and Applications*. Britain: Woodhead Publishing Series in Energy.

[7] Zhang, H. W., & Shen, P. K. (2012). Recent development of polymer electrolyte membranes for fuel cells. *Chem. Rev.,112(5)*, 2780–2832.

[8] Chandan, A., Hattenberger, M., Elkharouf, A., Du, S. F., Dhir, A., Self, V., *et al.* (2013). High temperature (HT) polymer electrolyte membrane fuel cells (PEMFC)—A review. *Journal of Power Sources, 231(12)*, 264–278.

[9] Orme, C. J., & Stewart, F. F. (2009). Pervaporation of water from aqueous sulfuric acid at elevated temperatures using Nafion® membranes. *Journal of Membrane Science, 326(2)*, 507–513.

[10] Orme, C. J., & Stewart, F. F. (2007). Pervaporation of water from aqueous hydriodic acid and iodine mixtures using Nafion® membranes. *Journal of Membrane Science, 304(1-2)*, 156–162.

[11] Stewart, F. F., Orme, C. J., & Jones, M. G. (2007). Membrane processes for the sulfur-iodine thermochemical cycle. *Int. J. Hydrogen Energy, 32(4)*, 457–462.

[12] Wycisk, R., Ballengee, J., & Pintauro, P. N. (2013). Polymer membranes for fuel cells. In E. M. V. Hoek, & V. V. Tarabara (Eds.), *Encyclopedia of Membrane Science and Technology*. New York: Wiley-Blackwell.

[13] Sportsman, K. S., Way, J. D., Chen, W. J., Pez, G.P., & Laciak, D. V. (2002). The dehydration of nitric acid using pervaporation and a nafion perfluorosulfonate/perfluorocarboxylate bilayer membrane. *Journal of Membrane Science, 203(1-2)*, 155–166.

[14] Chen, Zan, Li, Y. H., Yin, D. H., Song, Y. M., Ren, X. X., Lu, J. M., *et al.* (2012). Microstructural optimization of mordenite membrane for pervaporation dehydration of acetic acid. *Journal of Membrane Science, 411–412*, 182–192.

[15] Mah, S. K., Chai, S. P., & Wu, T. Y. (2014). Dehydration of glycerin solution using pervaporation: HybSi and polydimethylsiloxane membranes. *Journal of Membrane Science, 450*, 440–446.

[16] Lang, W. Z., Tong, W., Xu, Z. L., Guo, Y. J. (2010). Preparation of PFSA/PSf hollow fiber composite membranes with recovered PFSA for the pervaporation separation of EtOH/H_2O. *Science China Chemistry, 53(1)*, 273–280.

[17] Bolto, B., Hoang, M., Xie, & Z. L. (2011). A review of membrane selection for the dehydration of aqueous ethanol by pervaporation. *Chemical Engineering and Processing: Process Intensification, 50(3)*, 227–235.

[18] Guo, H., Kasahara, S., Tanaka, N., & Onuki, K. (2012). Energy requirement of HI separation from HI–I_2–H_2O mixture using electro-electrodialysis and distillation. *International Journal of Hydrogen Energy, 37(19)*, 13971–13982.

[19] Jiang, J. S., Greenberg, D. B., & Fried, J. R. (1997). Pervaporation of methanol from a triglyme solution using a Nafion membrane: 2. concentration polarization. *Journal of Membrane Science ,132*, 263–271.

[20] Zhang, H. W., & Shen, P. K. (2012). Advances in the high performance polymer electrolyte membranes for fuel cells. *Chem. Soc. Rev., 41(6)*, 2382-2394.

[21] Chen, Z., Yin, D. H., Li, Y. H., Yang, J. H., Lu, J. M., Zhang, Y., *et al.* (2011). Functional defect-patching of a zeolite membrane for the dehydration of acetic acid by pervaporation. *Journal of Membrane Science, 369 (1–2)*, 506–513.

[22] Pereira, C. C., Ribeiro, J. C. P., Nobrega, R., & Borges, C. P. (2006). Review: Pervaporative recovery of volatile aroma compounds from fruit juices. *Journal of Membrane Science, 274(1)*, 1–23.

[23] Rao, A. S., Mohan, H. R., & Iskra, J. (2013). Hydrogen Peroxide. In L. A. Paquette(Ed.), *E-EROS Encyclopedia of Reagents for Organic Synthesis*. New York: John Wiley & Sons, Ltd.

[24] Parks, M., & Watling, D.(2004). The relationship between saturated hydrogen peroxide, water vapour and temperature. *Pharmaceutical Technology Europe*, 1-8.

[25] Jin, Y., Qiao, S., Zhang, L., Xu, Z. P., Smart, S., Costa, J. C. D., *et al.* (2008). Novel Nafion composite membranes with mesoporous silica nanospheres as inorganic fillers. *J. Power Sources, 185(2)*, 664–669.

Nguyen Huu Hieu was born in An Giang, Vietnam, in 1977. He received the B.S. degree in 2001 and M.S. degree in 2005 in Chemical Engineering from Ho Chi Minh University of Technology (HCMUT), Vietnam National University-HCMC. He got the Ph.D. degree in Chemical Engineering from Chonbuk National University, Korea, in 2012.

In 2012, he joined the Faculty of Chemical Engineering, HCMUT as a lecturer and became Deputy Director of Key Laboratory of Chemical Engineering and Petroleum Processing. His current research interests include graphene-based nanocomposite materials, membrane technology, technologies for renewable energy, natural products.